Medicina Universitaria 2009;**11(44)**:176-186

ELSEVIER

MEDICINA UNIVERSITARIA

www.elsevier.com.mx

REVIEW ARTICLE

Emerging cardiovascular molecular imaging approaches

Cory Siegel, MD,[1] Matthias Nahrendorf, MD, PhD,[1] Ralph Weissleder, MD, PhD.[1*]

[1]Center for Systems Biology and Harvard Medical School, Massachusetts General Hospital, Harvard Medical School, Boston, MA, United States of America.

Recibido: marzo, 2009. Aceptado: abril, 2009.

KEY WORDS
Cardiovascular; Molecular imaging; Nanotechnology; Fluorescence.

Abstract
New molecular imaging technologies, in particular optical ones, are increasingly used to understand the complexity and heterogeneity of cardiovascular diseases. While 'omic' approaches can provide us with comprehensive 'snapshots' of biomarkers, imaging studies can be used to understand the spatiotemporal activity of these markers *in vivo.* Imaging has also advanced clinically, and will ultimately allow us to determine disease activity and therapy response. In addition, newer developments will likely have an impact on our understanding of biology at the systems level, promote earlier clinical diagnosis and accelerate drug development.

PALABRAS CLAVE
Cardiovascular;
Imagen molecular;
Nanotecnología;
Fluorescencia

Nuevas técnicas moleculares de imagen cardiovascular

Resumen
Nuevas tecnologías de imagen molecular, en particular las denominadas ópticas, están siendo usadas con mayor frecuencia para entender lo complejo y heterogéneo de las enfermedades cardiovasculares. Por un lado el acercamiento "proteómico" nos provee imágenes completas e "instantáneas" de biomarcadores de un padecimiento, y los estudios de imagen pueden ser usados para entender la actividad en el espacio y tiempo de estos marcadores *in vivo.* Las imágenes también han avanzado clínicamente, lo que finalmente nos permitirá determinar la actividad de un padecimiento y su respuesta al tratamiento. Además, los nuevos desarrollos probablemente tendrán un impacto en nuestra comprensión de la biología de estos sistemas, promoviendo el desarrollo de métodos de diagnostico temprano y poder acelerar el desarrollo de drogas.

**Corresponding author:* Ralph Weissleder, MD PhD. MGH-CSB, CPZN-5206 185. Cambridge. Street Boston, MA 02124. Telephone: 617-726-8226. Fax: 617-726-5708.*E mail:* rweissleder@mgh.harvard.edu

Table 1. Selected Targeted Cardiovascular Molecular Imaging Agents

Biologic Process	Target	Agent	Modality
Atherosclerosis	Macrophages	MLP's	MRI
		MPO-Gd	MRI
		N1177	CT
		64Cu-TNP	Pet. MRI, Optical
		^{18}F-CLIO	Pet. MRI, Optical
	Proteases	Prosense, MMPsense	Optical
	VCAM-1	VINP-28	MRI, Optical
Thrombosis	Fibrin	EP-2104R	MRI
Myocardial Infarction	Apoptosis	AnxCLIO	MRI, Optical
	Factor XIII	FXIII-111In	SPECT
	Macrophages	CLIO-VT680	MRI, Optical

MNP: Magnetic nanoparticles; MPO: Myeloperoxidase; Gd: Gadolinium; CLIO: Cross-linked iron oxide; VCAM-1: Vascular cell adhesion molecule-1; VINP-28: VCAM-1 internalizing nanoparticle-28.

Introduction

Prevention and early detection are increasingly important components of clinical cardiovascular care, because preventive strategies can save lives and are more cost effective. To implement these strategies, sensitive, specific and molecular-based imaging tools are needed that allow timely and specific diagnosis and risk stratification. A number of emerging molecular imaging techniques promise to achieve these goals, based on technological advances of equipment and the development of new imaging probes. Biomarkers of disease severity include inflammation, thrombosis, apoptosis, necrosis, remodeling, and angiogenesis, all common to diverse diseases such as atherosclerosis, myocardial infarction, heart failure, and stroke.

Several recent reviews have described molecular imaging of cardiovascular disease.[1-6] This review aims to complement and update with a focus on emerging imaging strategies that show the greatest promise and those likely to be rapidly translated into clinical practice.

Preclinical advances

A wide array of cardiovascular molecular imaging applications is about to emerge from preclinical advances. Novel agents have been developed that report on specific molecular targets, increasing the sensitivity and specificity of existing imaging modalities (**Table 1**). The keys to a successful reporter in this regard are twofold. One aspect must be a sensitive detection mechanism, while the other is targeting the desired biologic process via affinity ligand binding or reporter activation. Successful agents often harness amplification strategies such as chemical ones (increased relaxivity of magnetic nanoparticles, fluorescence dequenching) or biological ones (cellular trapping, pretargeting). Advances in nanotechnology now allow for the attachment of multiple ligands for heightened affinity, as well as multiple reporters per nanoparticle. In the cardiovascular imaging arena, the most commonly used detection platforms are magnetic resonance imaging (MRI), computed tomography (CT), positron emission tomography (PET), single photon emission computed tomography (SPECT), and fluorescence imaging such as fluorescence molecular tomography (FMT) and catheter based sensors (fluorescence, optical coherence tomography -OCT-).

Magnetic resonance imaging

Magnetic resonance imaging does not involve ionizing radiation, and provides good anatomic detail with outstanding tissue contrast. It allows for relative quantification of targets and is a very versatile technology. It uses inherent amplification mechanisms, since not the reporter itself, but rather its interaction with many surrounding protons is detected. Molecular MRI relies on 2 major classes of agents: T1-type probes that contain paramagnetic gadolinium (Gd) chelates, and T2 -type magnetic nanoparticles. While the latter mostly decrease the proton signal in T2 weighted sequences, newer approaches are being explored to overcome the disadvantage of signal decay, such as bright iron techniques.[7, 8] Clinical molecular MRI has also been successful: for instance, a fibrin sensing gadolinium chelate was used to image vascular thrombotic complications[9] (**Figure 1**). Here, the relative abundance of the imaging target affords sufficient sensitivity. Other appro-

Figure 1. In vivo MR imaging with fibrin-specific contrast agent, EP-2104R.

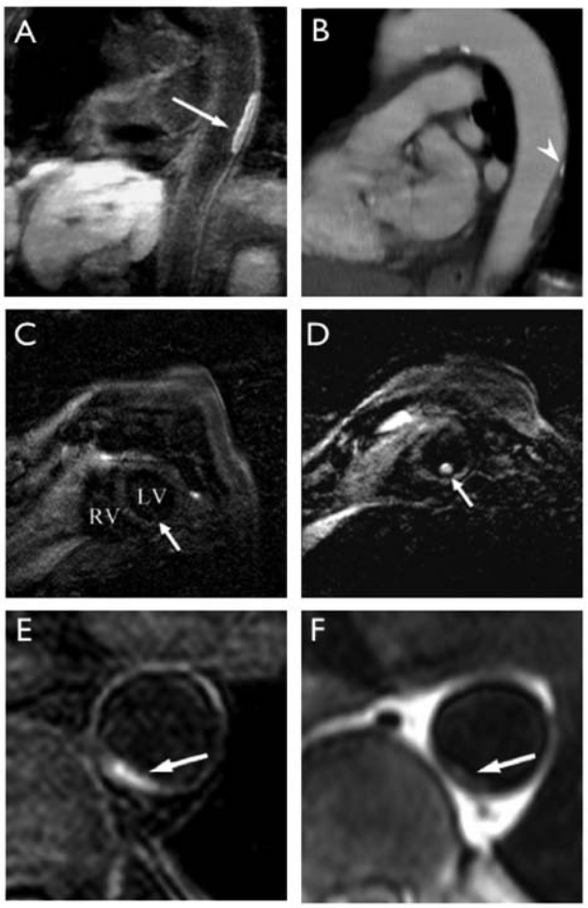

A Post EP2104R injection inversion recovery black-blood gradient-echo imaging (IR) sagittal cut of thrombus (arrow) in descending thoracic aorta of 82-year-old female patient compared to conventional CT multiplanar reconstruction **B** In image B, white arrowhead delineates a calcification. **C** and **D** Pre- and post- contrast cross-sectional imaging of left ventricular thrombus (arrows) in an 80-year-old male patient using IR (RV: right ventricle, LV: left ventricle). **E** Descending thoracic aorta thrombus (arrow) in 65-year-old male patient with EP-2104R contrast and pre-contrast T2-weighted black-blood turbo spin imaging **F** Adapted with permission.[9]

aches for sensitive T1 targeted imaging involve signal amplification through activatable Gd-chelates[10] (**Figure 2**).

Recently, although Gd-DTPA has been used for decades, there has been concern over the risk of nephrogenic systemic fibrosis (NSF), a disorder associated with the use gadolinium-based contrast agents in patients with renal insufficiency.[11]Therefore, techniques that reduce the required quantity of gadolinium and increase detection sensitivity are of great interest. Ultrasmall superparamagnetic nanoparticles with sufficient T1 effects such as fermoxytol have been proposed as alternatives to gadolinium based contrast agents for vascular imaging in renally-impaired patients where there is concern for NSF.[12]

Magnetic nanoparticles

The high relaxivity of magnetic nanoparticles make them a promising platform for molecular MRI. Here, the propensity of these particles to be taken up by innate immune phagocytes[13] is exploited. This allows for effective targeting and high contrast, particularly in the imaging of inflammatory cells in conditions such as atherosclerosis,[14, 15] infarction,[16, 17] and transplant rejection.[18, 19] However, large amounts of nanoparticles are often required to target macrophages (> 5 mg Fe/kg). For example, Korosoglou *et al* 2008 were able to identify macrophage laden atherosclerotic plaques in rabbits with the use of monocrystalline iron-oxide nanoparticles (MION-47) and an MRI method known as inversion recovery with ON-resonant water suppression (IRON)-MRI (**Figure 3**). One limitation of this study was the use of a total iron dose of 500 µmol Fe/kg, equivalent to a dose of 13 mg Fe/kg, well above the recommended dose of the FDA.[7] However, superparamagnetic nanoparticles have been used for clinical imaging of cancer metastasis[20] and in patients with atherosclerotic lesions in the carotid arteries.[21,22]

A variety of preclinical studies have explored the versatility of nanoparticles for targeted imaging by attaching affinity ligands to the shell of nanoparticles.[15, 23] The size, physical properties, attachment of affinity ligands, and conjugation to fluorochromes are all characteristics of an expanding library of nanoparticles that allow for customization of these particles to specific clinical needs. For example, the cross-linked, aminated surface of the magnetic nanoparticle CLIO-47 allows for the attachment of fluorochromes, and thus the potential for MR-optical imaging with magneto-fluorescent nanoparticles (MFNPs). The MNFP conjugate CLIO-VT680 has been used for macrophage targeting, quantification of cellular distribution on MFNP's, and MR sensing of inflammation in mouse atheromata.[14] MR-optical imaging has also been used in the targeting of apoptotic processes, using annexin as an affinity ligand for phosphatidylserine in the cell membrane, an early marker for apoptosis. The annexin-V-based nanoparticle AnxCLIO acts as a reporter for both MR and NIRF and has been used in vivo to identify regions of cardiomyocyte apoptosis in mice.[24] Annexin has also been used to target apoptosis with SPECT imaging in animal models[25-28] and patients,[29] and shows promise in PET imaging with ^{18}F-labelled annexin.[30]

The cell surface adhesion molecule VCAM-1 has also been used as a target for MNP's,[15, 31, 32] given its expression on activated endothelial cells, smooth muscle cells, and macrophages early in the inflammatory process of atherosclerotic plaques.[33, 34]

Among the next generation of magnetic nanoparticles are carboxymethyl dextran nanoparticles, some of which are already seeing clinical use. Ferumoxytol is an example of this, and already has been shown to have a favorable safety profile in phase I and II clinical trials for use as iron-replacement therapy in anemia.[35,36] As it was

Figure 2. Targeted MR imaging of myeloperoxidase (MPO) activity using an activatible MPO-Gd chelate in injured myocardium in mice.

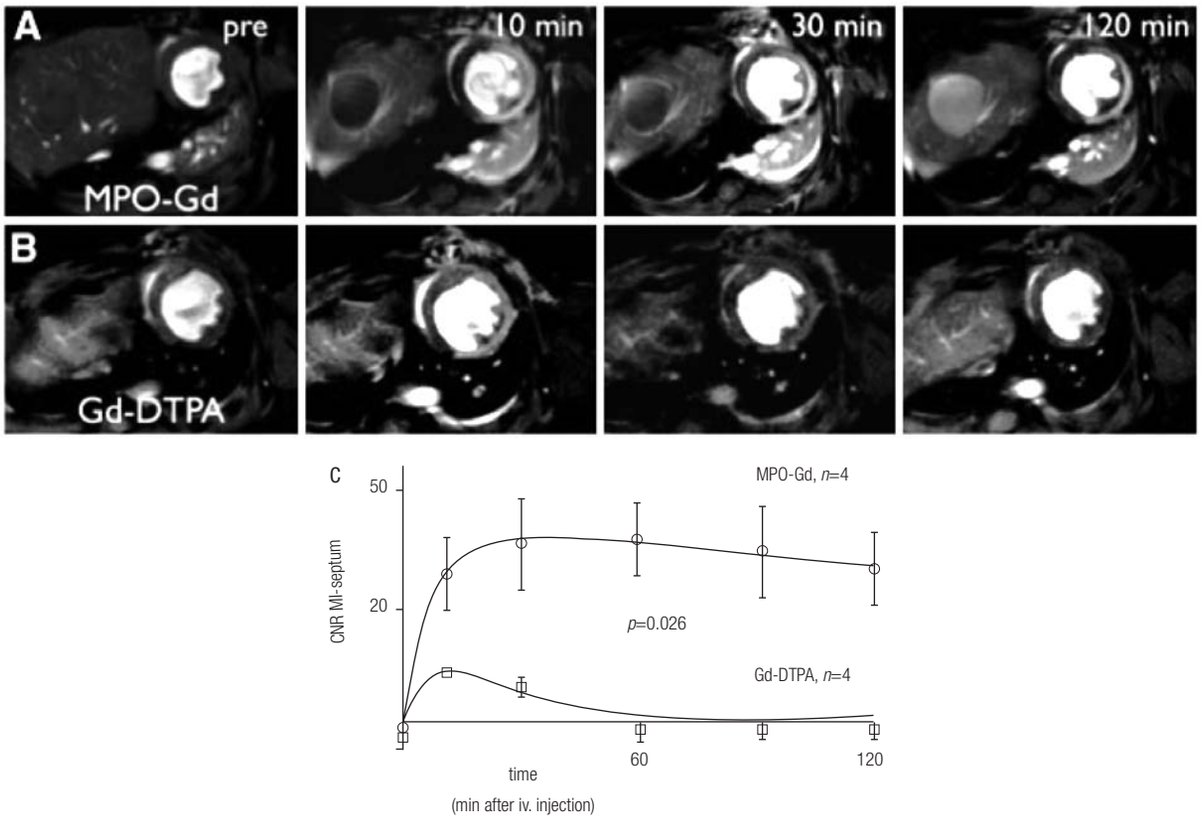

A Time course of MPO-Gd signal showing bright and persistent signal enhancement over 2 hours on day 2 after MI. **B** Conventional MR imaging with Gd-DTPA over same time period, showing progressive reduction in signal intensity over the 2 hour period. **C** Graphical representation comparing contrast-to-noise ratios (CNR) for MPO-Gd and Gd-DTPA imaging of the myocardial septum showing longer duration of high signal with MPO-Gd. Adapted with permission[10]

designed specifically for anemia therapy in patients with chronic kidney disease, it retains its favorable safety profile in patients with chronic renal impairment. It has characteristics that improve upon the prior generation prototype, ferumoxtran-10, which was successful in several clinical trials.[20-22] With a blood half-life of 10-14 hours, increased signal in the vasculature secondary to a greater T1 shortening, and the ability to be given as an injectable bolus, ferumoxytol is among the more promising of this generation of nanoparticles. Recent patient studies reveal applications in the identification of malignant lymph node metastasis by MR,[37] for imaging of brain tumors[38] and as a vascular contrast agent for use in MR angiography.[38-40] Ultrasmall superparamagnetic particles have also been shown to have a role in imaging of atherosclerotic plaques in both animal and patient studies.[41-44]

Gadolinium-based agents

One of the interesting examples for clinical molecular MRI is the fibrin-specific contrast agent EP-2104R. Originally tested in several animal models,[45-51] it has advanced to a Phase II study in human subjects with known intra-cardiac or intra-arterial thrombi.[9] This compound is a small peptide with 4 Gd-chelate moieties that binds to fibrin, but not to circulating fibrinogen.[52] Results show that in the majority of patients, signal enhancement of the thrombus was visualized with high contrast to the background tissue, and when compared with precontrast imaging (**Figure 1**).[9] Additionally, based on data from animal studies, this technique could be useful for detection of pulmonary embolism and deep vein thrombosis.

Another recent innovation using MRI uses a "smart" gadolinium chelate sensitive to the activity of myeloperoxidase (MPO), an enzyme known to be present in high levels within atherosclerotic plaque and produced by macrophages and neutrophils.[53] The agent is activated by radicalization in the presence of MPO, and then undergoes polymerization resulting in increased T1 relaxivity. The activated agent also crosslinks to surrounding proteins, effectively trapping the molecule in areas of high MPO

Figure 3. MR atherosclerotic plaque detection using monocrystalline iron-oxide nanoparticles (MION-47).

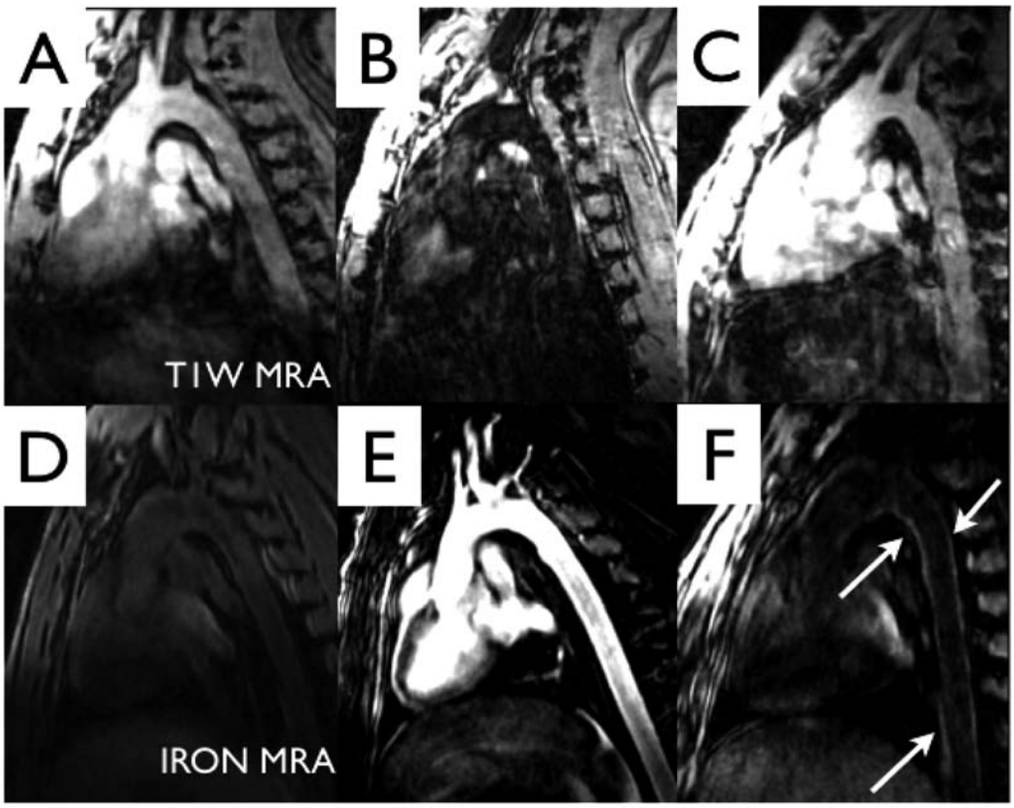

A-C Conventional T1W MRA of hyperlipidemic rabbits pre-injection **A**, immediately post-injection (day 0) **B**, and on day 6 after injection of MION-47 **C**. Signal decrease in **B** secondary to T2*-shortening of blood. **D-F** Inversion recovery with ON-resonant water suppression (IRON) MRA of the thoracic aorta before and after injection of MION-47 in hyperlipidemic rabbits. **D** IRON MRA of thoracic aorta pre-injection of MION-47. **E** IRON MRA immediately post-injection (day 0) of MION-47 and **F** IRON MRA on day 6 after injection identifying atherosclerotic lesions in the aorta (arrows). Adapted with permission[7]

activity, all of which results in increased enhancement on T1-weighted MRI.[53] We have shown the agent enables detection of MPO activity in infarcted myocardium (**Figure 2**) and allows for the monitoring of atorvastatin's anti-inflammatory effects.[10] This demonstrates the agent's potential for detection of myocardial inflammation and monitoring of pharmaceutical response. Recently, the agent was used to visualize cerebral inflammation secondary to stroke.[54] Given the increased myeloperoxidase activity in atherosclerotic plaque,[55] it is also an attractive modality to image vulnerable inflammatory atherosclerotic lesions.

Computed tomography

There have been few targeted contrast agents for CT, most likely due to the low sensitivity of this modality. Therefore, CT has been primarily employed in hybrid imaging to add anatomical information to PET, CT and optical sensing. However recently, Hyafil et al described a nanoparticulate contrast agent for CT, N1177. This compound is composed of crystalline iodinated particles dispersed with surfactant that targets macrophages in atherosclerotic plaques, potentially enhancing the use of CT for identification of at-risk inflammatory lesions.[56] The nanoparticulate formulation achieved a signal amplification that allowed molecular sensing in these experiments. An important aspect of this work is that coronary CT currently has the technological edge when it comes to resolution; however, radiation exposure needs to be carefully balanced against the benefits of screening.[57]

Nuclear imaging

Nuclear imaging modalities such as SPECT and PET potentially have high sensitivity for detecting reporters at low concentrations.[58] PET imaging is also fully quantitative, which facilitates efficient comparison of imaging

Figure 4. ^{18}FDG PET/CT imaging of human aortic atherosclerosis.

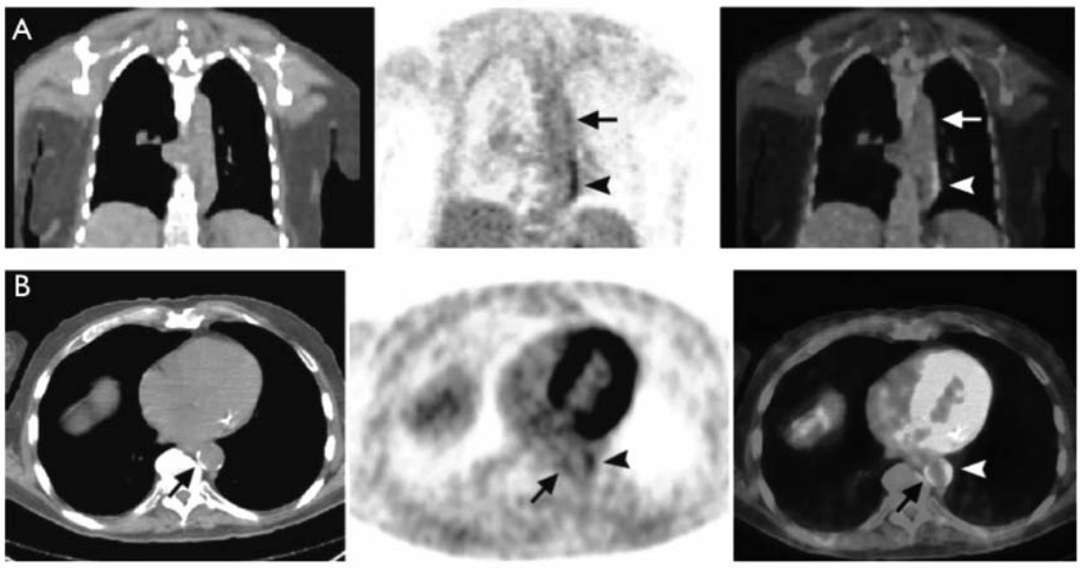

A Coronal CT (left), PET (middle) and fused PET/CT (right) images showing ^{18}FDG uptake (arrow/arrowheads) in descending thoracic aorta. **B** Transaxial CT (left), PET (middle), and fused PET/CT (right) images showing ^{18}FDG uptake in descending thoracic aorta (arrow/arrowheads). Note high background uptake in myocardium of left ventricle. Adapted with permission[72]

Figure 5. PET/CT imaging for macrophages using labeled nanoparticles.

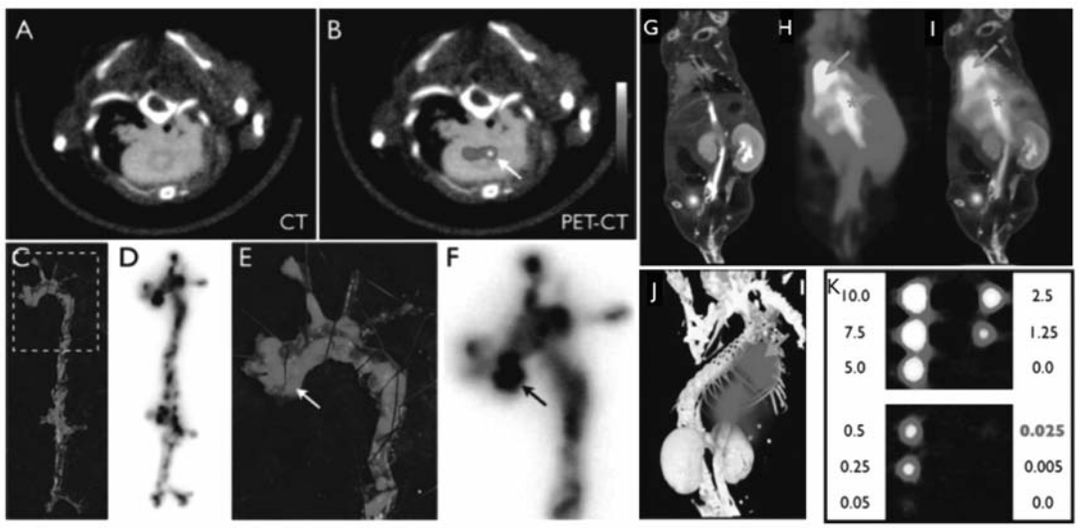

A-F Multimodality ^{64}Cu-TNP imaging of atherosclerosis in apoE$^{-/-}$ mouse. 64Cu-TNP distributes to atherosclerotic lesions. **A** and **B** PET-CT shows enhancement of the posterior aortic root (arrow). **C-F** En face Oil Red O staining of the excised aorta depicts plaque-loaded vessel segments, which colocalize with areas of high 64Cu-TNP uptake on autoradiography. **G-K** ^{18}F-CLIO imaging of mouse 2h after injection. **G** Coronal CT image. **H** Coronal PET image. **I** Fused PET/CT imaging. **J** 3D reconstruction of fused PET/CT images. **K** In vitro PET imaging of ^{18}F-CLIO showing detection threshold of 0.025μg Fe/mL. Liver ROI denoted by asterix and blood pool ROI by arrow. **A-F** adapted with permission.[58] **G-K** adapted with permission[78]

Figure 6. Enzyme activated fluorescent reporter and use in catheter-based NIRF detection.

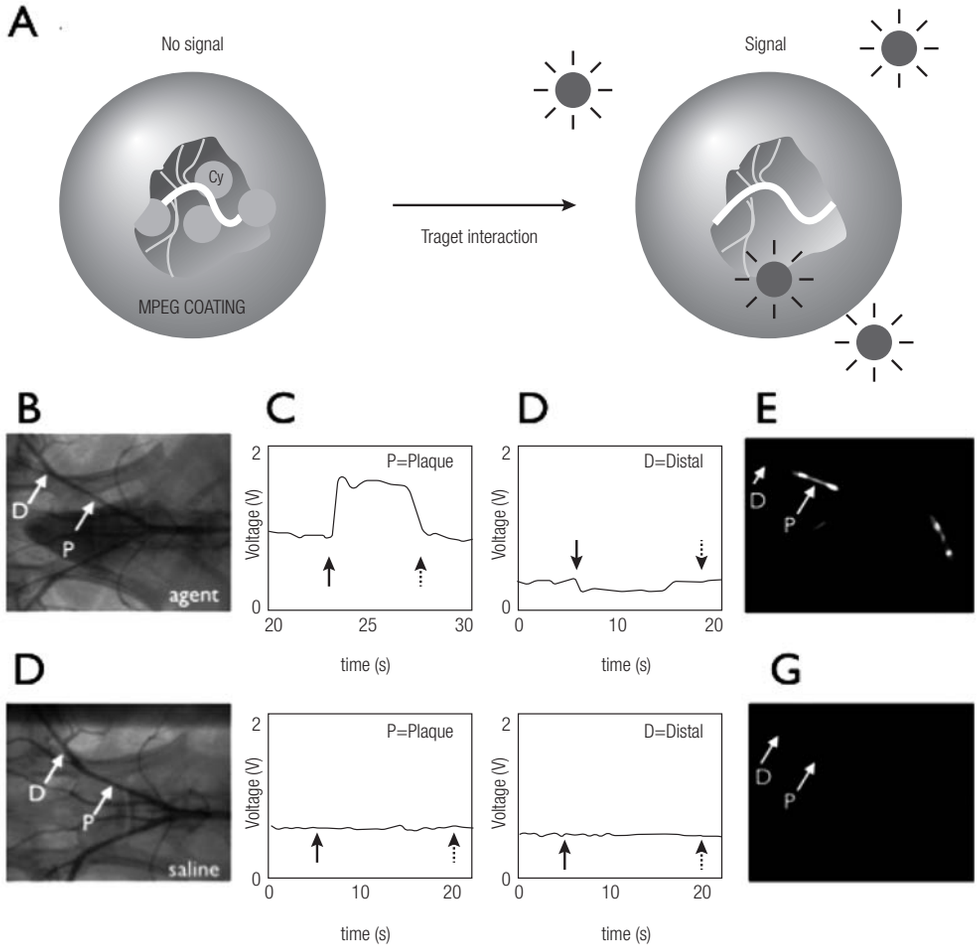

A Illustration of fluorescent reporter enzymatic activation in presence of a target. In the inactivated state, fluorochrome proximity quenches the fluorescent signal. Presence of the target enzyme releases the fluorochromes to an activated unquenched state. **B-G** In vivo intravascular catheter-based NIRF detection of atherosclerotic plaque in rabbits receiving protease NIR agent **B-E** and control rabbits **F-G**. **B** Conventional angiography of iliac vessels in rabbit receiving protease agent showing atherosclerosis. **C** NIR signal detected by intravascular NIRF catheter in region of atherosclerosis in rabbit receiving protease agent, and normal region **D** after balloon occlusion and saline flushing (area between arrows). The signal is reduced in **D** during flushing secondary to unactivated NIRF agent clearing. **E** Corresponding ex vivo NIRF image showing high signal in plaques but not in distal region. **F** Iliac angiography of control rabbit showing atherosclerotic plaque. **G** Catheter-based NIRF signal detection at atherosclerotic lesion and normal region (H) in control rabbit without presence of protease-sensitive agent. **H** NIRF ex-vivo image of iliac vessels showing minimal fluorescent signal in control rabbit. Adapted with permission[79, 82]

biomarkers longitudinally or between patient populations. However, these modalities provide little anatomic detail. Therefore, especially for imaging of small targets such as atherosclerotic plaques, both require localization with other modalities, such as CT or MRI. Clinical hybrid PET-CT systems are currently installed rapidly, and overcome the paucity of anatomical data in stand-alone nuclear imaging efficiently. To lower exposure to radionuclides, probes should have high affinity to their target and favorable, rapid pharmacokinetics that decrease exposure of vulnerable organs. For example, SPECT/CT was used to image monocyte trafficking to atherosclerotic lesions using an FDA-approved radiotracer, ^{111}In-oxine.[59] Additionally, in a study on transglutaminase activity in healing myocardial infarcts, it was possible to monitor Factor XIII activity in vivo using SPECT imaging with a Factor XIII

affinity peptide (^{111}In-DOTA-FXIII).[60] Progress in detection technology, especially in CT imaging, may also help to lower radiation dose. PET-MRI imaging is technically more challenging and therefore likely less cost effective, however, it offers anatomical information without adding radiation exposure as in PET-CT. Currently, and the first clinical PET-MRI systems are being installed.

18F-fludesoxiglucosa –FDG-

Since it is approved for oncologic imaging, ^{18}FDG-PET imaging has been a recent focus for cardiovascular imaging.^{18}FDG is a radio-labeled glucose analog that undergoes intracellular hexokinase-mediated phosphorylation after transport into metabolically active cells.[61] It is enriched in tissue with high metabolic activity, and therefore accumulates in cancer cells. Macrophages, key cells in atherosclerotic lesion development and complication,[62] also have rather high metabolic rates, therefore,^{18}FDG uptake has been proposed for imaging of atherosclerosis.[63, 64] Imaging with this tracer has already been performed in humans in multiple anatomic regions, including the carotid arteries,[65-69] peripheral arteries of upper[67] and lower[70] extremities, in addition to the aorta (**Figure 4**).[71, 72] Uptake of ^{18}FDG on PET imaging was described as correlating to the occurrence of cardiovascular events in patients,[73] and the signal intensity of ^{18}FDG-PET uptake in atherosclerotic plaques was attenuated by simvastatin therapy.[74] Yet, there are several limitations, including lack of specificity to atherosclerosis and accumulation in other metabolically active tissue. For example, imaging of the coronary arteries may prove difficult, as myocardium takes up ^{18}FDG readily (**Figure 4**). Also, imaging in the diabetic population is complicated and requires tight glucose and insulin control.[75] This is particularly problematic since diabetes is one of the major risk factors for atherosclerosis.

Nanoparticle positron emission tomography imaging

The use of macrophage-specific PET probes overcomes the problem of specificity and background signal seen in current ^{18}FDG-PET imaging. Recently, we described the development of macrophage-targeted PET agents utilizing long-circulating, dextran-coated nanoparticles.[58] The agent, ^{64}Cu-TNP, acts as a trimodality reporter in PET, MRI, and fluorescence, with a magnetic nanoparticle base conjugated to chelated ^{64}Cu and a near-infrared fluorochrome. In a mouse model of atherosclerosis, the detection threshold was 5 μg Fe/mL on T2-weighted MRI and 0.1 μg Fe/mL for PET-CT in the imaging phantom. The iron concentration used for PET imaging was 1.5mg Fe/kg, well below the maximum dose of magnetic nanoparticles approved by the FDA (2.6 mg Fe/kg). In apoE$^{-/-}$ mice, atherosclerotic plaques in the aorta were identified readily in-vivo on PET-CT (**Figure 5A-F**). This study used small amounts of ^{64}Cu and the copper was chelated, limiting its reactivity and toxicity. Additionally animal studies did not show evidence of toxicity for ^{64}Cu, which previously has been used in humans.[76, 77] Building further on this concept, we have also developed a trimodality reporter nanoparticle using ^{18}F labeled iron nanoparticles (^{18}F-CLIO). In contrast to ^{64}Cu, ^{18}F is readily available, has a greater PET detection sensitivity than ^{64}Cu and a shorter half-life, reducing the radiation exposure[78] (**Figure 5G-K**).

Optical imaging

Optical imaging is frequently used in preclinical research, since it is versatile, efficient and can be quantitative. The fluorochrome indocyanine green (ICG) is FDA approved for ophthalmic retinal angiography. Fluorochromes are non-toxic, and therefore promise to be of value for clinical translation. Near infrared wavelengths have the best properties for light transmission (< 8 cm) and autofluorescence is minimal at NIR wavelengths. We anticipate that fluorescent agents will play a major role for endoscopic and intraoperative imaging as well as for superficial structures, such as carotid arteries.

The use of fluorescent protease sensors for the identification and characterization of inflamed atherosclerotic lesions is highly promising. Matrix metalloproteinase (MMP) and cysteine protease activity increases in atherosclerotic plaques, and may be well suited to the identification of plaques at risk for rupture, given their enzymatic role in extracellular matrix degradation.[62] There are fluorescent reporters that minimally fluoresce in an inactivated quenched state, but when in proximity of proteases, undergo enzymatic cleavage and become highly fluorescent (**figure 6A**).[79] These reporters have been used in vivo to identify inflammatory atherosclerotic lesions.[80, 81] To use protease sensors in humans, an endovascular optical probe capable of detecting intravascular fluorescent signal is necessary.[82] We therefore developed a catheter system capable of detecting fluorescence and which has a floppy radiopaque tip (for simultaneous detection by x-ray angiography), and a maximum outer diameter of 0.48 mm.[82] Using a commercially available NIR protease sensitive fluorescent reporter, this catheter detects arterial atheromata in rabbits in vivo (**Figure 6B-G**). The study used vessels of similar caliber to human coronary arteries (rabbit iliac vessels), and a fluorescent reporter sensitive to the protease cathepsin B, which is associated with inflammation seen in atherosclerosis.[80, 83, 84]

Another optical modality seeing expanded use is optical coherence tomography (OCT). Similar in principle to ultrasound, but using infrared wavelengths, OCT achieves a high resolution (microns) and is able to penetrate several millimeters into tissue.[85] OCT for intravascular imaging of atherosclerosis has been suggested, and recently has been used to identify macrophages in atherosclerotic tissue using iron oxide nanoparticles.[86] It has also been used to explore intracoronary atherosclerotic lesions in human patients.[87-89] Combination of this technology with advances in molecular imaging techniques (i.e. molecular probes) may enable identification and characterization of vulnerable plaques.

Conclusion

Preclinical molecular imaging has developed a rich variety of targeted imaging tools, which are already accelerating basic research and drug development. While the field matures, it starts to focus on improved translatability of these techniques. Advantages of a given technique will have to be balanced with potential radiation exposure and probe toxicity, especially in preventive measures when relatively healthy patients are exposed. Promising clinical studies indicate that these goals can be achieved, and that clinical translation can enable early and specific diagnosis of diseases such as atherosclerosis and heart failure.

References

1. Jaffer FA, Libby P, Weissleder R. Molecular imaging of cardiovascular disease. Circulation 2007;116:1052-61.
2. Sinusas AJ. Multimodality cardiovascular molecular imaging, Part I. Circulation: Cardiovascular Imaging 2008;1:244-56.
3. Sanz J, Fayad ZA. Imaging of atherosclerotic cardiovascular disease. Nature 2008;451:953-7.
4. Jaffer FA, Libby P, Weissleder R. Molecular and cellular imaging of atherosclerosis: Emerging applications. J Am Coll Cardiol 2006;47:1328-38.
5. Nahrendorf M SD, French B, Swirski FK, *et al* Multimodality cardiovascular molecular imaging, Part II. Circ Cardiovasc Imaging 2009;2:56-70.
6. Choudhury RP, Fisher EA. Molecular imaging in atherosclerosis, thrombosis, and vascular inflammation. Arterioscler Thromb Vasc Biol July 1, 2009; 29(7): 981-2.
7. Korosoglou G, Weiss RG, Kedziorek DA, *et al*.Noninvasive detection of macrophage-rich atherosclerotic plaque in hyperlipidemic rabbits using "positive contrast" magnetic resonance imaging. J Am Coll Cardiol 2008;52:483-91.
8. Farrar CT, Dai G, Novikov M, et al Impact of field strength and iron oxide nanoparticle concentration on the linearity and diagnostic accuracy of off-resonance imaging. NMR Biomed 2008;21:453-63.
9. Spuentrup E, Botnar RM, Wiethoff AJ, et al. MR imaging of thrombi using EP-2104R, a fibrin-specific contrast agent: initial results in patients Eur Radiol. 2008;18:1995-2005.
10. Nahrendorf M, Sosnovik D, Chen JW, et al. Activatable magnetic resonance imaging agent reports myeloperoxidase activity in healing infarcts and noninvasively detects the antiinflammatory effects of atorvastatin on ischemia-reperfusion injury. Circulation 2008;117:1153-60.
11. Shellock FG, Spinazzi A. MRI safety update 2008: part 1, MRI contrast agents and nephrogenic systemic fibrosis. AJR Am J Roentgenol 2008;191:1129-39.
12. Neuwelt EA, Hamilton BE, Varallyay CG, et al. Ultrasmall superparamagnetic iron oxides (USPIOs): a future alternative magnetic resonance (MR) contrast agent for patients at risk for nephrogenic systemic fibrosis (NSF)? Kidney Int 2009;75:465-74.
13. Sosnovik DE, Nahrendorf M, Weissleder R. Magnetic nanoparticles for MR imaging: agents, techniques and cardiovascular applications. Basic Res Cardiol 2008;103:122-30.
14. Jaffer FA, Nahrendorf M, Sosnovik D, Kelly KA, Aikawa E, Weissleder R. Cellular imaging of inflammation in atherosclerosis using magnetofluorescent nanomaterials. Mol Imaging 2006;5:85-92.
15. Nahrendorf M, Jaffer FA, Kelly KA, et al. Noninvasive vascular cell adhesion molecule-1 imaging identifies inflammatory activation of cells in atherosclerosis. Circulation 2006;114:1504-11.
16. Nahrendorf M, Sosnovik DE, Waterman P, et al. Dual channel optical tomographic imaging of leukocyte recruitment and protease activity in the healing myocardial infarct. Circ Res 2007;100:1218-25.
17. Sosnovik DE, Nahrendorf M, Deliolanis N, et al. Fluorescence tomography and magnetic resonance imaging of myocardial macrophage infiltration in infarcted myocardium in vivo. Circulation 2007;115:1384-91.
18. Kanno S, Wu YJ, Lee PC, et al. Macrophage accumulation associated with rat cardiac allograft rejection detected by magnetic resonance imaging with ultrasmall superparamagnetic iron oxide particles. Circulation 2001;104:934-8.
19. Christen T NM, Wildgruber M, Swirski FK, et al. Multimodal molecular imaging of innate immune cell function in transplant rejection. Circulation 2009;in press.
20. Harisinghani MG, Barentsz J, Hahn PF, et al. Noninvasive detection of clinically occult lymph-node metastases in prostate cancer. N Engl J Med 2003;348:2491-9.
21. Trivedi RA, JM UK-I, Graves MJ, et al. In vivo detection of macrophages in human carotid atheroma: temporal dependence of ultrasmall superparamagnetic particles of iron oxide-enhanced MRI. Stroke 2004;35:1631-5.
22. Kooi ME, Cappendijk VC, Cleutjens KB, et al. Accumulation of ultrasmall superparamagnetic particles of iron oxide in human atherosclerotic plaques can be detected by in vivo magnetic resonance imaging. Circulation 2003;107:2453-8.
23. Weissleder R, Kelly K, Sun EY, Shtatland T, Josephson L. Cell-specific targeting of nanoparticles by multivalent attachment of small molecules. Nat Biotechnol 2005;23:1418-23.
24. Sosnovik DE, Schellenberger EA, Nahrendorf M, et al. Magnetic resonance imaging of cardiomyocyte apoptosis with a novel magneto-optical nanoparticle. Magn Reson Med 2005;54:718-24.
25. Johnson LL, Schofield L, Donahay T, Narula N, Narula J. 99mTc-annexin V imaging for in vivo detection of atherosclerotic lesions in porcine coronary arteries. J Nucl Med 2005;46:1186-93.
26. Isobe S, Tsimikas S, Zhou J, et al. Noninvasive imaging of atherosclerotic lesions in apolipoprotein E-deficient and low-density-lipoprotein receptor-deficient mice with annexin A5. J Nucl Med 2006;47:1497-505.
27. Kolodgie FD, Petrov A, Virmani R, et al. Targeting of apoptotic macrophages and experimental atheroma with radiolabeled annexin V: a technique with potential for noninvasive imaging of vulnerable plaque. Circulation 2003;108:3134-9.
28. Sarai M, Hartung D, Petrov A, et al. Broad and specific caspase inhibitor-induced acute repression of apoptosis in atherosclerotic lesions evaluated by radiolabeled annexin A5 imaging. J Am Coll Cardiol 2007;50(24):2305-2312.
29. Kietselaer BL, Reutelingsperger CP, Heidendal GA, et al. Noninvasive detection of plaque instability with use of radiolabeled annexin A5 in patients with carotid-artery atherosclerosis. N Engl J Med 2004;350:1472-3.
30. Murakami Y, Takamatsu H, Taki J, et al. 18F-labelled annexin V: a PET tracer for apoptosis imaging. Eur J Nucl Med Mol Imaging 2004;31:469-74.
31. Kelly KA, Allport JR, Tsourkas A, Shinde-Patil VR, Josephson L, Weissleder R. Detection of vascular adhesion molecule-1 expression using a novel multimodal nanoparticle. Circ Res 2005;96:327-36.
32. Tsourkas A, Shinde-Patil VR, Kelly KA, et al. In vivo imaging of activated endothelium using an anti-VCAM-1 magnetooptical probe. Bioconjug Chem 2005;16:576-81.
33. Cybulsky MI, Gimbrone MA, Jr. Endothelial expression of a mononuclear leukocyte adhesion molecule during atherogenesis. Science 1991;251:788-91.

34. O'Brien KD, Allen MD, McDonald TO, et al. Vascular cell adhesion molecule-1 is expressed in human coronary atherosclerotic plaques. Implications for the mode of progression of advanced coronary atherosclerosis. J Clin Invest 1993;92:945-51.
35. Landry R, Jacobs PM, Davis R, Shenouda M, Bolton WK. Pharmacokinetic study of ferumoxytol: a new iron replacement therapy in normal subjects and hemodialysis patients. Am J Nephrol 2005;25:400-10.
36. Spinowitz BS, Schwenk MH, Jacobs PM, et al. The safety and efficacy of ferumoxytol therapy in anemic chronic kidney disease patients. Kidney Int 2005;68:1801-7.
37. Harisinghani M, Ross RW, Guimaraes AR, Weissleder R. Utility of a new bolus-injectable nanoparticle for clinical cancer staging. Neoplasia 2007;9:1160-5.
38. Neuwelt EA, Varallyay CG, Manninger S, et al. The potential of ferumoxytol nanoparticle magnetic resonance imaging, perfusion, and angiography in central nervous system malignancy: a pilot study. Neurosurgery 2007;60:601-11; discussion 611-602.
39. Ersoy H, Jacobs P, Kent CK, Prince MR. Blood pool MR angiography of aortic stent-graft endoleak. AJR Am J Roentgenol 2004;182:1181-6.
40. Li W, Tutton S, Vu AT, et al. First-pass contrast-enhanced magnetic resonance angiography in humans using ferumoxytol, a novel ultrasmall superparamagnetic iron oxide (USPIO)-based blood pool agent. J Magn Reson Imaging 2005;21:46-52.
41. Durand E, Raynaud JS, Bruneval P, et al. Magnetic resonance imaging of ruptured plaques in the rabbit with ultrasmall superparamagnetic particles of iron oxide. J Vasc Res 2007;44:119-28.
42. Herborn CU, Vogt FM, Lauenstein TC, et al. Magnetic resonance imaging of experimental atherosclerotic plaque: comparison of two ultrasmall superparamagnetic particles of iron oxide. J Magn Reson Imaging. 2006;24:388-93.
43. Ruehm SG, Corot C, Vogt P, Kolb S, Debatin JF. Magnetic resonance imaging of atherosclerotic plaque with ultrasmall superparamagnetic particles of iron oxide in hyperlipidemic rabbits. Circulation 2001;103:415-22.
44. Tang TY, Howarth SP, Miller SR, et al. Comparison of the inflammatory burden of truly asymptomatic carotid atheroma with atherosclerotic plaques in patients with asymptomatic carotid stenosis undergoing coronary artery bypass grafting: an ultrasmall superparamagnetic iron oxide enhanced magnetic resonance study. Eur J Vasc Endovasc Surg 2008;35:392-8.
45. Spuentrup E, Katoh M, Wiethoff AJ, et al. Molecular coronary MR imaging of human thrombi using EP-2104R, a fibrin-targeted contrast agent: experimental study in a swine model. Rofo 2007;179:1166-73.
46. Botnar RM, Buecker A, Wiethoff AJ, et al. In vivo magnetic resonance imaging of coronary thrombosis using a fibrin-binding molecular magnetic resonance contrast agent. Circulation 2004;110:1463-6.
47. Spuentrup E, Buecker A, Katoh M, et al. Molecular magnetic resonance imaging of coronary thrombosis and pulmonary emboli with a novel fibrin-targeted contrast agent. Circulation 2005;111:1377-82.
48. Spuentrup E, Fausten B, Kinzel S, et al. Molecular magnetic resonance imaging of atrial clots in a swine model. Circulation. 2005;112:396-9.
49. Stracke CP, Katoh M, Wiethoff AJ, Parsons EC, Spangenberg P, Spuntrup E. Molecular MRI of cerebral venous sinus thrombosis using a new fibrin-specific MR contrast agent. Stroke 2007;38:1476-81.
50. Sirol M, Aguinaldo JG, Graham PB, et al. Fibrin-targeted contrast agent for improvement of in vivo acute thrombus detection with magnetic resonance imaging. Atherosclerosis 2005;182:79-85.
51. Sirol M, Fuster V, Badimon JJ, et al. Chronic thrombus detection with in vivo magnetic resonance imaging and a fibrin-targeted contrast agent. Circulation. 2005;112:1594-600.
52. Spuentrup E, Katoh M, Buecker A, et al. Molecular MR imaging of human thrombi in a swine model of pulmonary embolism using a fibrin-specific contrast agent. Invest Radiol. 2007;42:586-95.
53. Chen JW, Querol Sans M, Bogdanov A, Jr., et al. Imaging of myeloperoxidase in mice by using novel amplifiable paramagnetic substrates. Radiology 2006;240:473-81.
54. Breckwoldt MO, Chen JW, Stangenberg L, et al. Tracking the inflammatory response in stroke in vivo by sensing the enzyme myeloperoxidase. Proc Natl Acad Sci U S A. 2008;105:18584-9.
55. Navab M, Anantharamaiah GM, Reddy ST, Van Lenten BJ, Ansell BJ, Fogelman AM. Mechanisms of disease: proatherogenic HDL--an evolving field. Nat Clin Pract Endocrinol Metab 2006;2:504-11.
56. Hyafil F, Cornily JC, Feig JE, et al. Noninvasive detection of macrophages using a nanoparticulate contrast agent for computed tomography. Nat Med. 2007;13:636-41.
57. Gerber TC, Carr JJ, Arai AE, et al. Ionizing radiation in cardiac imaging: a science advisory from the American Heart Association Committee on Cardiac Imaging of the Council on Clinical Cardiology and Committee on Cardiovascular Imaging and Intervention of the Council on Cardiovascular Radiology and Intervention. Circulation 2009;119:1056-65.
58. Nahrendorf M, Zhang H, Hembrador S, et al. Nanoparticle PET-CT imaging of macrophages in inflammatory atherosclerosis. Circulation. 2008;117:379-87.
59. Kircher MF, Grimm J, Swirski FK, et al. Noninvasive in vivo imaging of monocyte trafficking to atherosclerotic lesions. Circulation 2008;117:388-95.
60. Nahrendorf M, Aikawa E, Figueiredo JL, et al. Transglutaminase activity in acute infarcts predicts healing outcome and left ventricular remodelling: implications for FXIII therapy and antithrombin use in myocardial infarction. Eur Heart J 2008;29:445-54.
61. Smith TA. The rate-limiting step for tumor [18F]fluoro-2-deoxy-D-glucose (FDG) incorporation. Nucl Med Biol 2001;28:1-4.
62. Libby P. Inflammation in atherosclerosis. Nature 2002;420:868-74.
63. Kubota R, Yamada S, Kubota K, Ishiwata K, Tamahashi N, Ido T. Intratumoral distribution of fluorine-18-fluorodeoxyglucose in vivo: high accumulation in macrophages and granulation tissues studied by microautoradiography. J Nucl Med 1992;33:1972-80.
64. Deichen JT, Prante O, Gack M, Schmiedehausen K, Kuwert T. Uptake of [18F] fluorodeoxyglucose in human monocyte-macrophages in vitro. Eur J Nucl Med Mol Imaging 2003;30:267-73.
65. Rudd JH, Warburton EA, Fryer TD, et al. Imaging atherosclerotic plaque inflammation with [18F]-fluorodeoxyglucose positron emission tomography. Circulation. 2002;105:2708-11.
66. Davies JR, Rudd JH, Fryer TD, et al. Identification of culprit lesions after transient ischemic attack by combined 18F fluorodeoxyglucose positron-emission tomography and high-resolution magnetic resonance imaging. Stroke. 2005;36:2642-7.

67. Okane K, Ibaraki M, Toyoshima H, et al. 18F-FDG accumulation in atherosclerosis: use of CT and MR co-registration of thoracic and carotid arteries. Eur J Nucl Med Mol Imaging 2006;33:589-94.
68. Tawakol A, Migrino RQ, Bashian GG, et al. In vivo 18F-fluorodeoxyglucose positron emission tomography imaging provides a noninvasive measure of carotid plaque inflammation in patients. J Am Coll Cardiol 2006;48:1818-24.
69. Arauz A, Hoyos L, Zenteno M, Mendoza R, Alexanderson E. Carotid plaque inflammation detected by 18F-fluorodeoxyglucose-positron emission tomography. Pilot study. Clin Neurol Neurosurg 2007;109:409-12.
70. Rudd JH, Myers KS, Bansilal S, et al. Atherosclerosis inflammation imaging with 18F-FDG PET: carotid, iliac, and femoral uptake reproducibility, quantification methods, and recommendations. J Nucl Med 2008;49:871-8.
71. Dunphy MP, Freiman A, Larson SM, Strauss HW. Association of vascular 18F-FDG uptake with vascular calcification. J Nucl Med 2005;46:1278-84.
72. Tatsumi M, Cohade C, Nakamoto Y, Wahl RL. Fluorodeoxyglucose uptake in the aortic wall at PET/CT: possible finding for active atherosclerosis. Radiology 2003;229:831-7.
73. Paulmier B, Duet M, Khayat R, et al. Arterial wall uptake of fluorodeoxyglucose on PET imaging in stable cancer disease patients indicates higher risk for cardiovascular events. J Nucl Cardiol 2008;15:209-17.
74. Tahara N, Kai H, Ishibashi M, et al. Simvastatin attenuates plaque inflammation: evaluation by fluorodeoxyglucose positron emission tomography. J Am Coll Cardiol 2006;48:1825-31.
75. Ghesani M, Depuey EG, Rozanski A. Role of F-18 FDG positron emission tomography (PET) in the assessment of myocardial viability. Echocardiography 2005;22:165-77.
76. Anderson CJ, Dehdashti F, Cutler PD, et al. 64Cu-TETA-octreotide as a PET imaging agent for patients with neuroendocrine tumors. J Nucl Med 2001;42:213-21.
77. Lewis JS, Connett JM, Garbow JR, et al. Copper-64-pyruvaldehyde-bis(N(4)-methylthiosemicarbazone) for the prevention of tumor growth at wound sites following laparoscopic surgery: monitoring therapy response with microPET and magnetic resonance imaging. Cancer Res 2002;62:445-9.
78. Devaraj NK, Keliher EJ, Thurber GM, Nahrendorf M, Weissleder R. (18)F Labeled Nanoparticles for in Vivo PET-CT Imaging. Bioconjug Chem 2009;20(2):397-401
79. Weissleder R, Tung CH, Mahmood U, Bogdanov A, Jr. In vivo imaging of tumors with protease-activated near-infrared fluorescent probes. Nat Biotechnol 1999;17:375-8.
80. Chen J, Tung CH, Mahmood U, Ntziachristos V, Gyurko R, Fishman MC, Huang PL, Weissleder R. In vivo imaging of proteolytic activity in atherosclerosis. Circulation 2002;105:2766-71.
81. Deguchi JO, Aikawa M, Tung CH, et al. Inflammation in atherosclerosis: visualizing matrix metalloproteinase action in macrophages in vivo. Circulation 2006;114:55-62.
82. Jaffer FA, Vinegoni C, John MC, et al. Real-time catheter molecular sensing of inflammation in proteolytically active atherosclerosis. Circulation 2008;118:1802-9.
83. Reddy VY, Zhang QY, Weiss SJ. Pericellular mobilization of the tissue-destructive cysteine proteinases, cathepsins B, L, and S, by human monocyte-derived macrophages. Proc Natl Acad Sci U S A 1995;92:3849-53.
84. Li W, Dalen H, Eaton JW, et al. Apoptotic death of inflammatory cells in human atheroma. Arterioscler Thromb Vasc Biol 2001;21:1124-30.
85. Raffel OC, Akasaka T, Jang IK. Cardiac optical coherence tomography. Heart 2008;94:1200-10.
86. Oh J, Feldman MD, Kim J, et al. Detection of macrophages in atherosclerotic tissue using magnetic nanoparticles and differential phase optical coherence tomography. J Biomed Opt 2008;13:054006.
87. Jang IK, Bouma BE, Kang DH, et al. Visualization of coronary atherosclerotic plaques in patients using optical coherence tomography: comparison with intravascular ultrasound. J Am Coll Cardiol 2002;39:604-9.
88. Tanaka A, Imanishi T, Kitabata H, et al. Distribution and frequency of thin-capped fibroatheromas and ruptured plaques in the entire culprit coronary artery in patients with acute coronary syndrome as determined by optical coherence tomography. Am J Cardiol 2008;102:975-9.
89. Tanaka A, Imanishi T, Kitabata H, et al. Morphology of exertion-triggered plaque rupture in patients with acute coronary syndrome: an optical coherence tomography study. Circulation 2008;118:2368-73.